

Red emission of additional Pr³⁺ and adjusting effect of additional Mg²⁺ in Ca₃Sc₂Si₃O₁₂:Ce³⁺, Mn²⁺ phosphor

Jun Qiao,^{1,2} Jiahua Zhang,^{1,*} Xia Zhang,¹ Zhendong Hao,¹ Yongfu Liu,³ and Guohui Pan¹

¹State Key Laboratory of Luminescence and Applications, Changchun Institute of Optics, Fine Mechanics and Physics, Chinese Academy of Sciences, 3888 Eastern South Lake Road, Changchun 130033, China

²University of Chinese Academy of Sciences, Beijing 100039, China

³Ningbo Institute of Materials Technology & Engineering, Chinese Academy of Sciences, Ningbo 315201, China

*Corresponding author: zhangjh@ciomp.ac.cn

Received February 26, 2014; revised March 27, 2014; accepted March 31, 2014;
published April 1, 2014 (Doc. ID 207233); published April 24, 2014

In this Letter, we report the addition of Pr³⁺ and Mg²⁺ in CSS:Ce³⁺, Mn²⁺ phosphor for improving the performances of white light-emitting diodes (LEDs). The additional trivalent Pr³⁺ will occupy the Ca²⁺ site in this host like the situation of Ce³⁺, its concentration can be enhanced by the addition of Mg²⁺ in Sc³⁺ site due to the substitution of Mg²⁺ for Sc³⁺ can compensate the charge mismatch between Pr³⁺ and Ca²⁺. Based on the efficient Ce³⁺ → Pr³⁺ and Mn²⁺ → Pr³⁺ energy transfers (ETs) and the compensation effect of Mg²⁺, the additional Pr³⁺ in our present phosphors exhibits an intense red-emission around 610 nm, which is significant for enhancing the color rendering property. In addition, we also find that the additional Mg²⁺ in Sc³⁺ site can markedly adjust the photoluminescence (PL) spectrum shape of our phosphor by controlling the distribution of Mn²⁺ at Ca²⁺ and Sc³⁺ sites. A new tunable full-color emission is obtained via the ETs (Ce³⁺ → Mn²⁺, Ce³⁺ → Pr³⁺ and Mn²⁺ → Pr³⁺) and the adjusting effect of Mg²⁺ in our present phosphors. Finally, a white LED with higher color rendering index of 90, lower correlated color temperature of 4980 K, and chromaticity coordinates of (0.34, 0.31) was obtained by combining the single CSS:0.08Ce³⁺, 0.01Pr³⁺, 0.3Mn²⁺, 0.2Mg²⁺ phosphor with a blue-emitting InGaN LED chip. © 2014 Optical Society of America

OCIS codes: (160.2540) Fluorescent and luminescent materials; (300.6280) Spectroscopy, fluorescence and luminescence; (160.4670) Optical materials; (230.3670) Light-emitting diodes.

<http://dx.doi.org/10.1364/OL.39.002691>

White light-emitting diodes (LEDs) are considered to be a promising candidate for the future lighting system [1]. The most widely used white LED consists of a blue-emitting InGaN LED chip and Y₃Al₅O₁₂:Ce³⁺ (YAG:Ce³⁺) yellow phosphor. However, this type of white LED emits little red light and therefore has a relatively low color rendering index (CRI) [2]. To solve this problem, the method of mixing green and red phosphors instead of YAG:Ce³⁺ phosphor has been proposed [3,4]. Unfortunately, phosphor mixture gives fluorescence re-absorption that results in loss of luminous efficiency. Therefore, to achieve single phase phosphor with full color emission is expected. The attempt to enhance the red emission component in YAG:Ce³⁺ was performed by codoping Pr³⁺ on Y³⁺ site to generate a red emission line around 610 nm, originated from ¹D₂ → ³H₄ transition of Pr³⁺ through Ce³⁺ → Pr³⁺ energy transfer (ET) [5]. A new yellow-emitting Ba_{0.93}Eu_{0.07}Al₂O₄ phosphor with sufficient red component was also synthesized by Li *et al.* Warm-white emissions with correlated color temperature (CCT) < 4000 K and CRI > 80 were readily achieved when combining this phosphor with a blue LED (440–470 nm) [6].

Shimomura *et al.* reported a novel green-emitting Ca₃Sc₂Si₃O₁₂:Ce³⁺ (CSS:Ce³⁺) phosphor with higher thermal stability and luminous intensity [7]. In this host lattice, the concentration of Ce³⁺ that occupies the Ca²⁺ site can be enhanced by the substitution of Mg²⁺ for Sc³⁺ due to the charge compensation effect, resulting in a remarkable redshift of the Ce³⁺ emission band [8]. In our previous work, we have introduced Mn²⁺ into CSS:Ce³⁺ to enrich the longer wavelength visible emission through Ce³⁺ → Mn²⁺ ET. It was demonstrated that Mn²⁺ may occupy not only the Ca²⁺ site to generate a yellow emis-

sion around 574 nm [named Mn²⁺(I)] but also the Sc³⁺ site to generate a red emission around 680 nm [named Mn²⁺(II)]. However, the white LEDs obtained by combining this phosphor with a blue InGaN LED chip have lower CRI (below 80) [9]. For enhancing the color rendering property, we tentatively introduced Pr³⁺ and Mg²⁺ to modify this phosphor. It is found that the additional Pr³⁺ in CSS:Ce³⁺, Mn²⁺ phosphor can generate a distinct red emission around 610 nm through obvious Ce³⁺ → Pr³⁺ and Mn²⁺(I) → Pr³⁺ ETs besides slender direct excitation when exciting our phosphor with blue light. Furthermore, we also found that the addition of Mg²⁺ in Sc³⁺ site can markedly modify the photoluminescence (PL) spectrum shape of our phosphor for improving the chromaticity properties of white LEDs.

In this Letter, we report Ce³⁺ → Pr³⁺ and Mn²⁺(I) → Pr³⁺ ETs besides Ce³⁺ → Mn²⁺ [Mn²⁺(I) and Mn²⁺(II)] ETs in our present phosphors. The adjustment for PL spectra is performed through the addition of Mg²⁺ in the Sc³⁺ site in this host. A white LED with CRI of 90 and CCT of 4980 K is obtained by combining the single CSS:0.08Ce³⁺, 0.01Pr³⁺, 0.3Mn²⁺, 0.2Mg²⁺ phosphor with a blue-emitting InGaN LED chip.

The samples were synthesized by conventional solid-state reaction. Mixtures of raw materials were sintered in a tubular furnace at 1350°C for 4 h in reductive atmosphere (5%H₂ + 95%N₂). The PL and PL excitation (PLE) spectra were measured using a HITACHI F-7000 spectrometer. The chromaticity coordinates, CRI, CCT, and luminous efficiency of white LED were measured using an Ocean Optics USB4000 spectrometer.

Figures 1(a)–1(c) show PLE and PL spectra for CSS:0.05Ce³⁺, CSS:0.2Mn²⁺, and CSS:0.01Pr³⁺, respectively. CSS:0.05Ce³⁺ exhibits a green PL band with a peak

at 505 nm and a shoulder around 540 nm, originated from the transitions of Ce^{3+} from 5d to ${}^2\text{F}_{5/2}$ and ${}^2\text{F}_{7/2}$ [7]. The relevant PLE spectrum appears an intense excitation band around 450 nm, well matching the emitting wavelength of blue InGaN LEDs. CSS:0.2Mn^{2+} exhibits two emission bands, one is a yellow emission band around 574 nm [Mn^{2+} (I)] and the other one is a red emission band around 680 nm [Mn^{2+} (II)], assigned to ${}^4\text{T}_1(4\text{G}) \rightarrow {}^6\text{A}_1(6\text{S})$ transitions of Mn^{2+} ions that substitute for Ca^{2+} and Sc^{3+} sites, respectively. The relevant PLE spectra show typical forbidden d-d transitions of Mn^{2+} , resulting in very weak luminous intensities compared with Ce^{3+} in CSS [9]. CSS:0.01Pr^{3+} exhibits a red emission around 610 nm, originated from ${}^1\text{D}_2 \rightarrow {}^3\text{H}_4$ transition of Pr^{3+} . The PLE spectrum monitored at 610 nm includes three bands, the band peaked around 285 nm is ascribed to ${}^3\text{H}_4 \rightarrow 4\text{f}5\text{d}$ transitions of Pr^{3+} , the band in the range of 430–500 nm is attributed to ${}^3\text{H}_4 \rightarrow {}^3\text{P}_{0,1,2}$ and ${}^3\text{H}_4 \rightarrow {}^1\text{I}_6$ transitions of Pr^{3+} , and the band in the range of 570–600 nm is assigned to ${}^3\text{H}_4 \rightarrow {}^1\text{D}_2$ transitions of Pr^{3+} [10,11]. The luminous intensity of Pr^{3+} is also very weak in comparison with the strong emission of Ce^{3+} in CSS.

Figures 1(d) and 1(e) show PL spectra for CSS:0.05Ce^{3+} , 0.01Pr^{3+} and $\text{CSS:0.2Mn}^{2+} x\text{Pr}^{3+}$ ($x = 0, 0.01$). The PL spectrum for CSS:0.05Ce^{3+} , 0.01Pr^{3+} upon Ce^{3+} excitation at 406 nm exhibits not only the Ce^{3+} emission band around 505 nm but also the Pr^{3+} emission around 610 nm. This feature proves the occurrence of distinct $\text{Ce}^{3+} \rightarrow \text{Pr}^{3+}$ ET, which can be clearly understood as noticing the spectral overlap between the Ce^{3+} emission band and the Pr^{3+} excitation band in CSS. For CSS:0.2Mn^{2+} , 0.01Pr^{3+} , the PL spectrum upon Mn^{2+} excitation at 406 nm appears not only the Mn^{2+} emission bands around 574 and 680 nm but also the Pr^{3+} emission around 610 nm. Considering the extent of spectral overlap between the Mn^{2+} [Mn^{2+} (I) and Mn^{2+} (II)] emission bands and the Pr^{3+} excitation band in CSS, we infer that

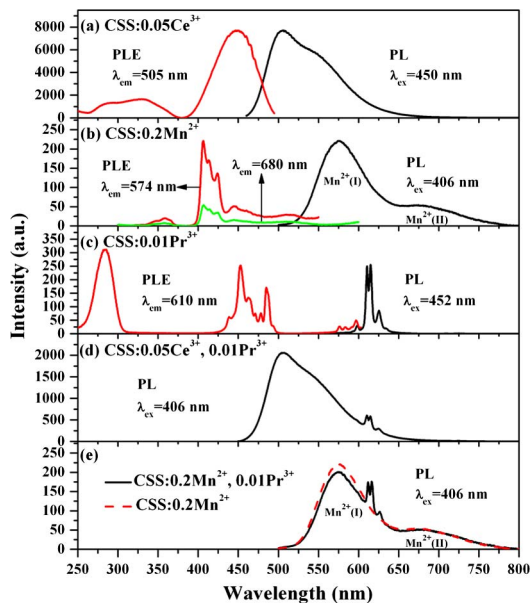


Fig. 1. PLE and PL spectra for (a) CSS:0.05Ce^{3+} , (b) CSS:0.2Mn^{2+} , and (c) CSS:0.01Pr^{3+} ; PL spectra for (d) CSS:0.05Ce^{3+} , 0.01Pr^{3+} and (e) CSS:0.2Mn^{2+} , $x\text{Pr}^{3+}$ ($x = 0, 0.01$).

the excitation of Pr^{3+} is likely performed by ET from Mn^{2+} (I) rather than Mn^{2+} (II). In order to prove our inference, we have seriously compared the PL spectra of CSS:0.2Mn^{2+} and CSS:0.2Mn^{2+} , 0.01Pr^{3+} in Fig. 1(e), the emission intensity of Mn^{2+} (I) in presence of Pr^{3+} distinctly decreases compared with that of Mn^{2+} (I) in absence of Pr^{3+} , meanwhile, the emission intensity of Mn^{2+} (II) almost remains unchanged. This feature effectively proves that the excitation of Pr^{3+} is performed mainly by the ET from Mn^{2+} (I) rather than Mn^{2+} (II).

Figure 2(a) shows the normalized PL spectra ($\lambda_{\text{ex}} = 435 \text{ nm}$) for CSS:0.05Ce^{3+} , 0.01Pr^{3+} , 0.3Mn^{2+} , $y\text{Mg}^{2+}$. For the phosphor without Mg^{2+} , the PL spectrum exhibits a distinct red-emission of additional Pr^{3+} around 610 nm besides the green band of Ce^{3+} , the yellow band of Mn^{2+} (I), and the red band of Mn^{2+} (II). Considering that the emissions of Mn^{2+} [Mn^{2+} (I) and Mn^{2+} (II)] and Pr^{3+} are very weak under direct excitation and the excitation wavelength of 435 nm is outside of the optimal excitation wavelength ranges for Mn^{2+} [Mn^{2+} (I) and Mn^{2+} (II)] and Pr^{3+} ; the relatively remarkable emissions of Mn^{2+} [Mn^{2+} (I) and Mn^{2+} (II)] in present phosphors should be mainly attributed to ETs from Ce^{3+} rather than direct excitation, and the distinct emission of Pr^{3+} in present phosphors is mainly attributed to ETs from Ce^{3+} and Mn^{2+} (I) rather than direct excitation. As shown in Fig. 2(b), based on these ETs, we obtained full-color emission in our present phosphors. However, this phosphor still has deficient emission around 610 nm, which limits its color rendering performance. In order to optimize the luminescence properties of our present

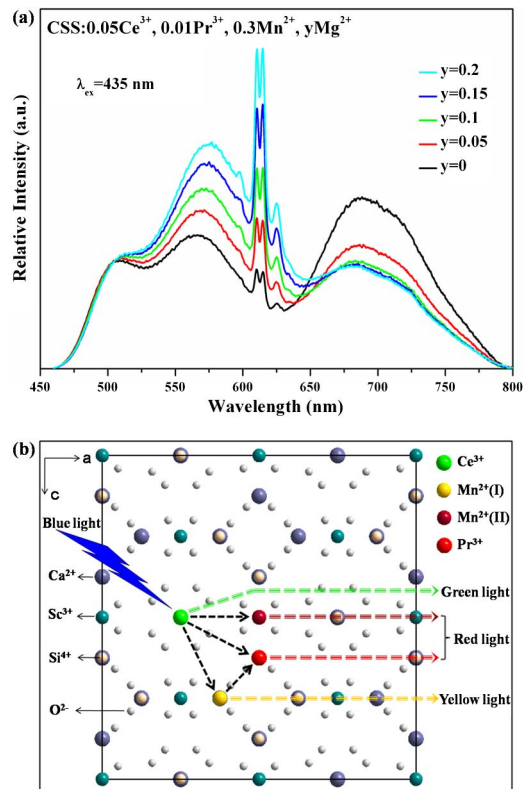


Fig. 2. (a) PL spectra for CSS:0.05Ce^{3+} , 0.01Pr^{3+} , 0.3Mn^{2+} , $y\text{Mg}^{2+}$ and (b) the schematic for ETs in schematic crystal structure of present phosphors under excitation by blue light.

phosphor, the addition of Mg^{2+} that substitutes for Sc^{3+} is performed. It is observed that the effect of additional Mg^{2+} on modifying the PL spectra shape is very significant, especially the Pr^{3+} emission around 610 nm is remarkably enhanced with increasing the nominal Mg^{2+} content. For the purpose of understanding this modification, it is necessary to study the effect of additional Mg^{2+} on the emissions of Ce^{3+} , Pr^{3+} , and Mn^{2+} in our phosphors, respectively. Therefore, the samples with nominal compositions of CSS:0.05Ce^{3+} , $y\text{Mg}^{2+}$, CSS:0.01Pr^{3+} , $y\text{Mg}^{2+}$, and CSS:0.3Mn^{2+} , $y\text{Mg}^{2+}$ ($y = 0-0.2$) have been prepared separately.

Figure 3 shows the PL spectra for CSS:0.05Ce^{3+} , $y\text{Mg}^{2+}$ ($\lambda_{\text{ex}} = 450$ nm), CSS:0.01Pr^{3+} , $y\text{Mg}^{2+}$ ($\lambda_{\text{ex}} = 452$ nm), and CSS:0.3Mn^{2+} , $y\text{Mg}^{2+}$ ($\lambda_{\text{ex}} = 406$ nm) under appropriate light excitation. With increasing Mg^{2+} content, the redshift of Ce^{3+} emission in CSS:0.05Ce^{3+} , $y\text{Mg}^{2+}$ [Fig. 3(a)] and the enhancement of Pr^{3+} emission in CSS:0.01Pr^{3+} , $y\text{Mg}^{2+}$ [Fig. 3(b)] are probably attributed to the enhanced concentrations of Ce^{3+} and Pr^{3+} in these phosphors, respectively. The trivalent Ce^{3+} and Pr^{3+} both occupy the Ca^{2+} sites when they are incorporated into CSS lattices [7,12]. Their available lower concentrations, which are restrained by the charge mismatch between them and Ca^{2+} , can be enhanced by the substitution of Mg^{2+} for Sc^{3+} due to charge compensation effect. In the PL spectra for CSS:0.3Mn^{2+} , $y\text{Mg}^{2+}$ [Fig. 3(c)], with increasing Mg^{2+} content, the Mn^{2+} (I) emission continuously enhances as the Mn^{2+} (II) emission obviously weakens. The possible reason is that the incorporation of Mg^{2+} into the Sc^{3+} site in CSS restrains the formation of Mn^{2+} (II) that substitutes for Sc^{3+} due to the competitive relation between them, so that more Mn^{2+} in raw material can be incorporated into the Ca^{2+} site to be Mn^{2+} (I).

According to the above analysis, the modification caused by the additional Mg^{2+} for the PL spectra ($\lambda_{\text{ex}} = 435$ nm) of CSS:0.05Ce^{3+} , 0.01Pr^{3+} , 0.3Mn^{2+}

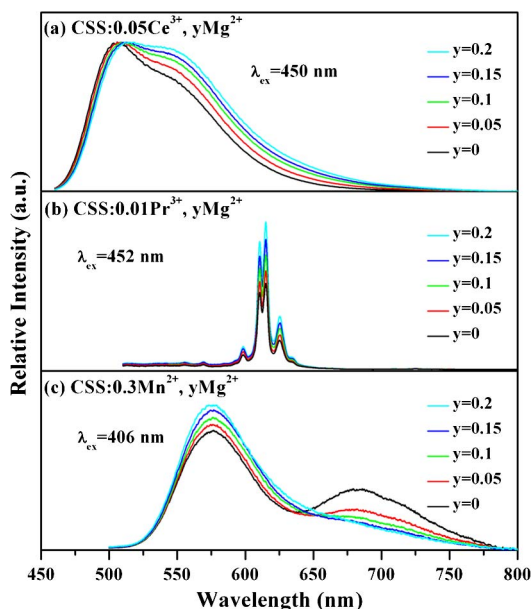


Fig. 3. PL spectra for (a) CSS:0.05Ce^{3+} , $y\text{Mg}^{2+}$, (b) CSS:0.01Pr^{3+} , $y\text{Mg}^{2+}$, and (c) CSS:0.3Mn^{2+} , $y\text{Mg}^{2+}$.

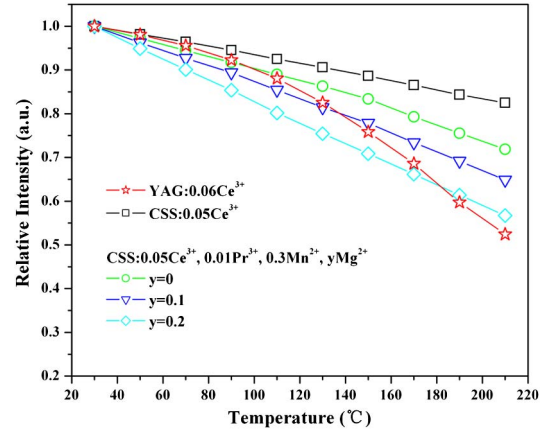


Fig. 4. Temperature dependence of integral PL intensity of YAG:0.06Ce^{3+} , CSS:0.05Ce^{3+} , and CSS:0.05Ce^{3+} , 0.01Pr^{3+} , 0.3Mn^{2+} , $y\text{Mg}^{2+}$ under excitation at 450 nm.

can be understood as follows: with increasing Mg^{2+} content, the enhancement of the yellow emission band is comprised of the redshift of the Ce^{3+} emission and the enhancement of Mn^{2+} (I) emission. The redshift of Ce^{3+} emission is mainly attributed to the increasing concentration of Ce^{3+} , as reported by Shimomura *et al.* [8]. The enhancement of Mn^{2+} (I) emission is mainly attributed to the enhanced $\text{Ce}^{3+} \rightarrow \text{Mn}^{2+}$ (I) ET efficiency, which is caused by the increasing concentration of Mn^{2+} (I). The remarkable enhancement of Pr^{3+} emission around 610 nm is mainly attributed to the enhanced $\text{Ce}^{3+} \rightarrow \text{Pr}^{3+}$ and Mn^{2+} (I) $\rightarrow \text{Pr}^{3+}$ ET efficiencies, which are caused by the increasing concentration of Pr^{3+} . Meanwhile, the reduction of the Mn^{2+} (II) emission band around 680 nm is mainly attributed to the decreasing $\text{Ce}^{3+} \rightarrow \text{Mn}^{2+}$ (II) ET efficiency, which is caused by the decreasing concentration of Mn^{2+} (II).

Temperature-quenching characteristics of YAG:Ce^{3+} and our present phosphors are presented in Fig. 4, in which the integral PL intensity at 30°C is set as the normalized standard. Apparently, the original CSS:0.05Ce^{3+} phosphor exhibits weaker thermal quenching compared with YAG:Ce^{3+} at the same temperature. With the additions of Pr^{3+} , Mn^{2+} , and Mg^{2+} in our present phosphors,

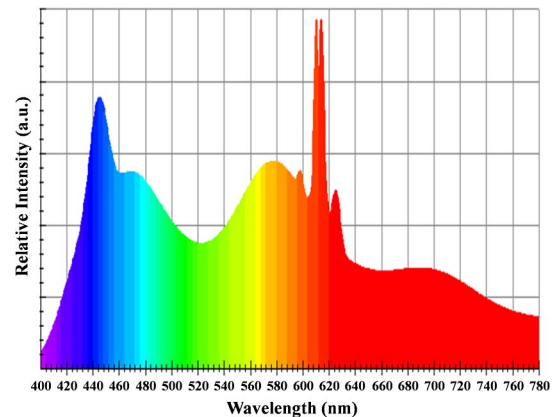


Fig. 5. Emission spectrum for the white LED fabricated by using the single CSS:0.08Ce^{3+} , 0.01Pr^{3+} , 0.3Mn^{2+} , 0.2Mg^{2+} phosphor and an InGaN LED ($\lambda = 445$ nm) chip. The current is 20 mA.

the thermal quenching behavior becomes significant due to the strong thermal quenching of Mn^{2+} and Pr^{3+} emissions, but on the whole, the emissions of our present phosphors still exhibit satisfactory thermal stability compared with that of $\text{YAG}:\text{Ce}^{3+}$.

For evaluating the chromaticity characteristics of our present phosphor, we have fabricated a white LED by combining our single $\text{CSS}:\text{0.08Ce}^{3+}$, 0.01Pr^{3+} , 0.3Mn^{2+} , 0.2Mg^{2+} phosphor with a blue-emitting InGaN LED chip (445 nm). Figure 5 shows the emission spectrum of our white LED. The luminous efficiency of our white LED can reach 26 lm/W while the generated white light exhibits a higher CRI of 90 and a lower CCT of 4980 K. These features demonstrate the potential application of our present phosphor for white LEDs with higher CRI and lower CCT.

In summary, we report the $\text{Ce}^{3+} \rightarrow \text{Pr}^{3+}$ and $\text{Mn}^{2+}(\text{I}) \rightarrow \text{Pr}^{3+}$ ETs in our present phosphor. The red emission of additional Pr^{3+} and the adjusting effect of additional Mg^{2+} in our present phosphors are very significant for obtaining phosphors with high performances. A white LED with luminous efficiency of 26 lm/W, CRI of 90, CCT of 4980 K, and chromaticity coordinates of (0.34, 0.31) is obtained by combining the single $\text{CSS}:\text{0.08Ce}^{3+}$, 0.01Pr^{3+} , 0.3Mn^{2+} , 0.2Mg^{2+} phosphor with a blue-emitting InGaN LED chip.

This work was supported by the National Natural Science Foundation of China (51172226, 61275055,

11274007, and 11174278) and the Natural Science Foundation of Jinlin province (201205024, 20140101169JC).

References

1. E. F. Schubert and J. K. Kim, *Science* **308**, 1274 (2005).
2. K. Bando, K. Sakano, Y. Noguchi, and Y. Shimizu, *J. Light Visual Environ.* **22**, 2 (1998).
3. R. J. Xie, N. Hirosaki, T. Suehiro, F. F. Xu, and M. Mitomo, *Chem. Mater.* **18**, 5578 (2006).
4. J. W. Li, T. Watanabe, N. Sakamoto, H. Wada, T. Setoyama, and M. Yoshimura, *Chem. Mater.* **20**, 2095 (2008).
5. H. S. Jang, W. B. Im, D. C. Lee, D. Y. Jeon, and S. S. Kim, *J. Lumin.* **126**, 371 (2007).
6. X. F. Li, J. D. Budai, F. Liu, J. Y. Howe, J. H. Zhang, X. J. Wang, Z. J. Gu, C. J. Sun, R. S. Meltzer, and Z. W. Pan, *Light: Sci. Appl.* **2**, e50 (2013).
7. Y. Shimomura, T. Honma, M. Shigeiwa, T. Akai, K. Okamoto, and N. Kijima, *J. Electrochem. Soc.* **154**, J35 (2007).
8. Y. Shimomura, T. Kurushima, M. Shigeiwa, and N. Kijima, *J. Electrochem. Soc.* **155**, J45 (2008).
9. Y. F. Liu, X. Zhang, Z. D. Hao, Y. S. Luo, X. J. Wang, and J. H. Zhang, *J. Mater. Chem.* **21**, 16379 (2011).
10. S. Pinelli, S. Bigotta, A. Toncelli, M. Tonelli, E. Cavalli, and E. Bovero, *Opt. Mater.* **25**, 91 (2004).
11. R. Piramidowicz, K. Ławniczuk, M. Nakielska, J. Sarnecki, and M. Malinowski, *J. Lumin.* **128**, 708 (2008).
12. K. V. Ivanovskikh, A. Meijerink, F. Piccinelli, A. Speghini, E. I. Zinin, C. Ronda, and M. Bettinelli, *J. Lumin.* **130**, 893 (2010).